MOX–Report No. 22/2012

Regression models for data distributed over non-planar domains

Ettinger, B.; Passerini, T.;Perotto, S.; Sangalli, L.M.

MOX, Dipartimento di Matematica "F. Brioschi"
Politecnico di Milano, Via Bonardi 9 - 20133 Milano (Italy)

mox@mate.polimi.it http://mox.polimi.it

Regression models for data distributed over non-planar domains

Bree Ettinger, Tiziano Passerini, Simona Perotto, Laura M. Sangalli

Abstract We consider the problem of surface estimation and spatial smoothing over non-planar domains. In particular, we deal with the case where the data or signals occur on a domain that is a surface in a three-dimensional space. The application driving our research is the modeling of hemodynamic data, such as the shear stress and the pressure exerted by blood flow on the wall of a carotid artery. The regression model we propose consists of two key phases. First, we conformally map the surface domain to a region in the plane. Then, we apply existing regression methods for planar domains, suitably modified to respect the geometry of the original surface domain.

Key words: Functional data analysis, penalized smoothing, conformal map, finite elements.

1 Introduction

In this paper, we deal with data that are observed over non-planar bi-dimensional domains. The motivating application is modeling the shear stress generated by the blood-flow over the wall of an internal carotid artery affected by an aneurysm. For instance, Figure 1 shows the geometry of a possible surface domain of interest: the observed values of the wall shear stress are shown by a color map over this domain. This type of data structure, where the quantity of interest is referred to a non-planar domain, occur in a number of different applications. Another fascinating

Bree Ettinger, Simona Perotto and Laura M. Sangalli
MOX - Dipartimento di Matematica "F. Brioschi," Politecnico di Milano, Piazza L. da Vinci 32, I-20133 Milano
e-mail: {bree.ettinger, simona.perotto, laura.sangalli}@polimi.it
Tiziano Passerini
Math & Science Center Emory University 400 Dowman Drive, W401, Atlanta, GA 30322
e-mail: tiziano@mathcs.emory.edu

application in the medical field is, e.g., the study of hemodynamic signals over the cortical surface. The environmental and geostatistical sciences also offer several applications that have this type of data structures.

Unfortunately, few methods are available for smoothing data over non-planar domains: essentially, the nearest neighbor averaging method (see, e.g., [6]) and the sophisticated heat kernel smoothing method proposed by [3]. Here, we adopt a Functional Data Analysis approach, and propose a regression method that efficiently handles these data structures. The proposed method consists of two steps: first we map the original surface domain to a flat domain, and then, properly modify existing spatial regression methods suited to deal with data on planar domains. In particular, to flatten the original surface domain we use a conformal map. The advantage of using of a conformal map, with respect to any other map, is that it preserves the angles in the original surface domain in the planar domain. The spatial regression method we use is the penalized least square estimation technique proposed in [15] and later generalized in [17]. The penalty is modified to account for the contribution of the conformal flattening map.

The paper is organized as follows. Section 2 describes the motivating applied problem in more detail. In Section 3, we first recall the spatial regression methods defined in [15] and then introduce the new approach. Section 4.1 provides a simple simulation study. In Section 4.2 we apply the proposed method to the study of hemodynamic data. Finally, in Section 5 we discuss possible extensions and future directions of the proposed approach.

2 Motivating applied problem

The research described in this section is motivated by the analysis of data within the AneuRisk Project, a scientific endeavor that investigates the pathogenesis of cerebral aneurysms, in an interdisciplinary effort combining the experience of practitioners from neurosurgery and neuroradiology with that of researchers from statistics, numerical analysis and bio-engineering. For a description of the AneuRisk Project, we refer the interested reader to the website http://ecm2.mathcs.emory.edu/aneurisk and references therein.

Cerebral aneurysms are deformations of cerebral vessels characterized by a bulge of the vessel wall. Figure 1 shows an example of an internal carotid artery, one of the main arteries bringing blood to the brain, affected by an aneurysm. The origin of aneurysms is considered to be the result of a complex interplay among systemic effects, the biomechanical properties of the vessel wall and the continuous effect of the forces exerted by the blood flow on the vessels. These hemodynamic forces depend on the vessel morphology itself. The study of these interactions and their role on the pathogenesis of aneurysms has been the main goal of the AneuRisk Project. The first studies available in literature on the pathology of aneurysms restricted their attention to the aneurysm sac. In constrast, the AneuRisk Project has investigated the morphological and hemodynamic features of the parent vasculature, i.e., the vessel

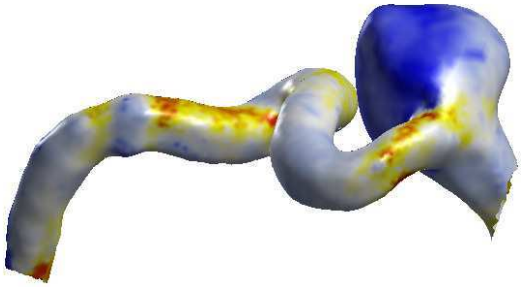

Fig. 1 Wall shear stress modulus at the systolic peak on a real internal carotid artery geometry affected by aneurysm (data from the AneuRisk project, http://ecm2.mathcs.emory.edu/aneurisk).

hosting the aneurysm and the upstream vasculature, with the goal of highlighting possible causes of aneurysm onset, development and rupture (see [10] and [18]).

In this paper, we analyze hemodynamic data on the real anatomy of internal carotid arteries. The internal carotid artery geometry is reconstructed from three-dimensional angiographic images, belonging to the AneuRisk data warehouse; for details on vessel geometry reconstruction see, e.g., [8]. The hemodynamic quantities, wall shear stress and pressure, have been simulated in [9] via Computational Fluid Dynamics. As detailed in [9] and [10], blood has been modeled as a Newtonian fluid, and its dynamics has been described by means of the incompressible Navier-Stokes equations. The geometry of the carotid artery has been assumed to be fixed in time, since compliance effects are expected to be negligible in this vascular district. Proper boundary conditions have been devised to ensure that the flow regime is comparable among all simulated cases. For each case, blood velocity and blood pressure have been simulated over three heart beats, and the wall shear stress has been computed in a post-processing step. Figure 1 shows the simulated wall shear stress modulus at the systolic peak on a real three-dimensional geometry. The hemodynamic data are referred to points (x, y, z) on the artery wall, the latter being a bidimensional, but not-planar, domain. In [2] and [17] some first analyses of these data were performed, by flattening a simplified version of the carotid domain. In particular, a new coordinate system is defined by (s, r, θ), where s is the curvilinear abscissa along the artery centerline, r the artery radius, and θ the angle of the surface point with respect to the artery centerline. The domain is then reduced to the plane $(s, \theta * \bar{r})$, where $\bar{r}$ is the average carotid radius on the carotid tract considered. This planar rectangular domain is essentially obtained by cutting the artery wall along the axial direction given by s and then opening and flattening the artery wall; notice that this planar domain is equivalent to a simplified three-dimensional artery geometry, where the radius is kept fixed to a constant value and the curvature of the artery is not taken into account. The map just described will be referred to in the following as the *angular map*. Then existing spatial regression methods for

the planar setting have been applied to the flattened simplified carotid geometry; in particular [17] employs Spatial Spline Regression (SSR) models. Notice that, by flattening the domain with the angular map and then applying a spatial regression method for planar domains, any information related to the vessel radius and curvature is lost; on the contrary, these two geometrical quantities greatly influence the hemodynamics in the artery and statistically discriminate aneurysm presence and location (see, e.g., [18]). Moreover, to have a bijective angular map, it is necessary to exclude the aneurysmal sac (otherwise, different points on the carotid wall would be mapped to the same point on the plane).

In the next section, after recalling Spatial Spline Regression (SSR) model for planar domains used in [17], we introduce the SSR model for non planar domains. This model allows us to consider the carotid geometry in its actual complexity, including the varying radius and curvature, and without need to remove of the aneurysmal sac.

3 Spatial Spline Regression Models

3.1 Spatial Spline Regression Model for planar domains

In this section, we present the Spatial Spline Regression models for planar domains introduced in [15] and the generalized version provided in [17] (see also [13] and [14]).

Let $\{\mathbf{u}_i = (u_i, v_i);\ i = 1, \ldots, n\}$ be a set of n data locations on a bounded regular domain $\Omega \subset \mathbb{R}^2$. Let w_i be the real valued variable of interest observed at point $\mathbf{u}_i$. Assume the model

$$w_i = f(\mathbf{u}_i) + \varepsilon_i \qquad\qquad i = 1, \ldots, n \tag{1}$$

where ε_i are independent observational errors with zero mean and constant variance, and f is a twice-differentiable real-valued function to be estimated. According to the SSR model, the estimate of f is found by minimizing the following functional

$$\sum_{i=1}^{n} (w_i - f(\mathbf{u}_i))^2 + \lambda \int_{\Omega} (\Delta f)^2 d\mathbf{u}, \tag{2}$$

i.e., a sum of squared errors penalized via the L^2-norm of the Laplacian of f. The Laplacian of f measures the local curvature of f. Hence in (2) via the penalty we are essentially controlling the roughness of the solution. Moreover, the Laplacian is invariant with respect to Euclidean transformations of the domain and this ensures that the smoothness of the estimate does not depend on the arbitrary chosen coordinate system.

The estimation problem (2) cannot be solved analytically. An approximate solution is found by resorting to a finite element approach, that provides a local basis for piecewise polynomial surfaces. The finite element method is largely employed

to approximate partial differential equations and it is widely used in engineering applications (for an introduction to the finite element framework see, e.g., [11]). The strategy is very similar to univariate splines. The finite element approach partitions the domain into small disjoint elements and then constructs a local polynomial function on each of these elements, in such a way that the union of these functions closely approximates the solution. This simplified problem becomes computationally tractable thanks to the suitable choice of the basis functions for the space of piecewise polynomials. Convenient domain partitions are provided by triangular meshes; see for instance Figure 2. A basis of piecewise polynomials is thus considered over a triangulation of the domain, the simplest being the one spanning the space of all the continuous functions which are linear when restricted to any triangle of the mesh. Thanks to the intrinsic construction of the finite element space, solving the estimation problem (2) reduces to solving a linear system. In particular, the estimator of f turns out to be linear with respect to the observed data values, so that classical inferential tools may be readily derived (see [17]).

3.2 Spatial Spline Regression Model for non-planar domains

Now consider the problem where the n data locations $\{\mathbf{x}_i = (x_i, y_i, z_i);\ i = 1, \ldots, n\}$ lie over a non-planar domain Σ, where Σ is a surface embedded in $\mathbb{R}^3$. For each location $\mathbf{x}_i$, a real valued random variable of interest, w_i, is observed. As in the planar case, we assume the model

$$w_i = f(\mathbf{x}_i) + \varepsilon_i \qquad\qquad i = 1, \ldots, n \tag{3}$$

where ε_i, $i = 1, \ldots, n$ are observational errors and f is now a function defined on the surface domain Σ; our aim is to estimate this function.

By analogy to (2), we propose to estimate f in (3) by minimizing the following penalized sum of squared error functional

$$J_\lambda(f(\mathbf{x})) = \sum_{i=1}^{n} (w_i - f(\mathbf{x}_i))^2 + \lambda \int_\Sigma (\Delta_\Sigma f(\mathbf{x}))^2 \, d\mathbf{x}, \tag{4}$$

where Δ_Σ is the Laplace-Beltrami operator for functions defined over the surface Σ. The Laplace-Beltrami operator is indeed the generalization of the common Laplacian: it can be used to operate on functions defined on surfaces in Euclidean spaces (see, e.g., [4]).

In [5] we show that it is possible to solve the estimation problem (4) by exploiting existing techniques over planar domains. In particular, we propose reducing (4) to a problem over a planar domain. To do this, we flatten Σ by means of a conformal map. Specifically, for the surface domain Σ we define a map X such that

$$\begin{aligned} X &: \Omega \to \Sigma \\ \mathbf{u} &= (u, v) \mapsto \mathbf{x} = (x, y, z) \end{aligned} \tag{5}$$

where Ω is an open, convex and bounded set in $\mathbb{R}^2$. Denote by $X_u(\mathbf{u})$ and $X_v(\mathbf{u})$ the column vectors of first order partial derivatives of X with respect to u and v. For the map X to be conformal, we require $\|X_u(\mathbf{u})\| = \|X_v(\mathbf{u})\|$ and $\langle X_u(\mathbf{u}), X_v(\mathbf{u})\rangle = 0$ where $\langle\cdot,\cdot\rangle$ denotes the standard Euclidean scalar product and $\|\cdot\|$ is the corresponding norm. Let us also define the (space-dependent) metric tensor as the following symmetric positive definite matrix

$$G(\mathbf{u}) := \begin{pmatrix} \|X_u(\mathbf{u})\|^2 & \langle X_u(\mathbf{u}), X_v(\mathbf{u})\rangle \\ \langle X_v(\mathbf{u}), X_u(\mathbf{u})\rangle & \|X_v(\mathbf{u})\|^2 \end{pmatrix} = \begin{pmatrix} g_{11}(\mathbf{u}) & g_{12}(\mathbf{u}) \\ g_{21}(\mathbf{u}) & g_{22}(\mathbf{u}) \end{pmatrix}$$

Then, the inverse metric tensor G^{-1} is given by

$$G^{-1}(\mathbf{u}) = \frac{1}{[\mathscr{W}(\mathbf{u})]^2} \begin{pmatrix} \|X_v(\mathbf{u})\|^2 & -\langle X_u(\mathbf{u}), X_v(\mathbf{u})\rangle \\ -\langle X_v(\mathbf{u}), X_u(\mathbf{u})\rangle & \|X_u(\mathbf{u})\|^2 \end{pmatrix} = \begin{pmatrix} g^{11}(\mathbf{u}) & g^{12}(\mathbf{u}) \\ g^{21}(\mathbf{u}) & g^{22}(\mathbf{u}) \end{pmatrix} \tag{6}$$

where $g^{12}(\mathbf{u}) = g^{21}(\mathbf{u})$ and $\mathscr{W}(\mathbf{u}) = \sqrt{\det(G(\mathbf{u}))}$. Note that the function $\mathscr{W}(\mathbf{u})$ is related to the change of variable (from $\mathbf{x}$ to $\mathbf{u}$) since the following holds for the area element: $d\mathbf{x} = \mathscr{W}(\mathbf{u})\, d\mathbf{u}$. Using this notation, for a function $f \circ X \in \mathscr{C}^2(\Omega)$, the Laplace-Beltrami operator associated with the surface Σ can be expressed as

$$\Delta_\Sigma f(\mathbf{x}) = \frac{1}{\mathscr{W}(\mathbf{u})} \sum_{i,j=1}^{2} \partial_i \left(g^{ij}(\mathbf{u})\, \mathscr{W}(\mathbf{u})\, \partial_j f(X(\mathbf{u})) \right) \tag{7}$$

where $\mathbf{u} = X^{-1}(\mathbf{x})$. Hence, in [5], we show that (4) can be equivalently expressed as the following problem over the planar domain Ω:

$$J_\lambda(f(X(\mathbf{u}))) = \\ \sum_{i=1}^{n} \left(w_i - f(X(\mathbf{u}_i))\right)^2 + \lambda \int_\Omega \left[\frac{1}{\mathscr{W}(\mathbf{u})} \sum_{i,j=1}^{2} \partial_i \left(g^{ij}(\mathbf{u})\, \mathscr{W}(\mathbf{u})\, \partial_j f(X(\mathbf{u})) \right) \right]^2 \mathscr{W}(\mathbf{u})\, d\mathbf{u} \tag{8}$$

where $X(\mathbf{u}_i) = \mathbf{x}_i$. Moreover, for conformal coordinates the functional J_λ reduces to

$$J_\lambda(f(X(\mathbf{u}))) = \sum_{i=1}^{n} \left(w_i - f(X(\mathbf{u}_i))\right)^2 + \lambda \int_\Omega \left(\frac{1}{\sqrt{\mathscr{W}(\mathbf{u})}}\, \Delta f(X(\mathbf{u})) \right)^2 d\mathbf{u} \tag{9}$$

where Δf is the standard Laplacian over the planar domain Ω. Therefore, this problem turns out to be a modification of the estimation problem presented in Section 3.1.

From a computational viewpoint, the conformal map in (5) may be approximated via non-planar finite elements. Non-planar finite elements are analogous to the finite elements mentioned in Section 3.1, except that the basis functions are defined over triangles of a three-dimensional triangular mesh. In [7] a non-planar finite element method is developed specifically for flattening tubular surfaces (in particular,

a portion of the colon). We resort to a similar approach since the wall of the carotid artery is indeed a tubular surface. The non-planar finite element method for approximating the conformal map starts with a three-dimensional triangular mesh that approximates the surface domain Σ. The three-dimensional mesh is then flattened via a conformal map into a planar triangular mesh that discretizes Ω. One benefit of using a conformal map is that it preserves angles and thus shapes, i.e., essentially, the triangulation.

Figure 2 illustrates the flattening of a test surface domain. Panel (a) shows the non-planar domain, a conoidal tubular surface, approximated by a three-dimensional triangular mesh, and panel (b) displays the conformally equivalent planar triangulated domain. In contrast, Figure 2, panel (c), shows the planar domain obtained with the angular map. The sides of the planar triangulation are labeled to have a correspondence with the surface in panel (a). In particular, the sides of the planar triangulation labeled with "bottom" and "top" correspond to the bottom and to the top open boundaries of the original three-dimensional domain. The two sides indicated by "cut" correspond to a cut along the three-dimensional domain, connecting the two open boundaries of the surface, that is computed when calculating the flattening map [7].

After the conformal flattening, we are ready to apply the modified estimation method (9). Note that the estimates along the two "cut" sides have to coincide; this is in fact an artificial cut. To prevent a seam, we have to take care to maintain the periodicity of the estimate along the "cut" edges (see [5], [2] and [17]). Similarly to SSR over planar domains, the estimator of f is linear with respect to the observed data values, so that classical inferential tools may be derived (see [5]).

4 Applications to simulated and real data

4.1 Simulations studies

In this section, we report the results of a first simulation study, illustrating the performance of the proposed smoothing technique over non-planar domains. In particular, we compare the results obtained via the proposed SSR model for non-planar domains with those yielded by the SSR model for planar domains combined with a simple angular flattening.

For these simulations, three domains, approximated by sufficiently fine three-dimensional triangular meshes, were considered; see Figure 3. Each geometry is obtained as a deformation of a circular cylinder. Over each of these non-planar domains, we consider 50 test functions, having the form $f(x,y,z) = a_1 \sin(2\pi x) + a_2 \sin(2\pi y) + a_3 \sin(2\pi z) + 1$ with coefficients a_i, for $i = 1,\ldots,3$, randomly generated from independent normal distributions with mean 1 and standard deviation 1. The data locations $\mathbf{x}_i$ coincide with the nodes of the three-dimensional meshes; each domain has 1648 data points. The noisy observations w_i in correspondence with the

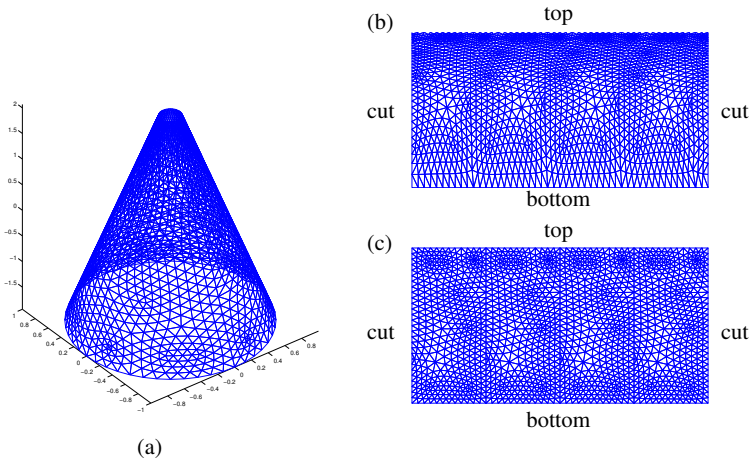

Fig. 2 Flattening of a non-planar domain: (a) three-dimensional triangular mesh approximating the non-planar domain consisting in a conoidal tubular surface, (b) planar triangulated domain obtained by conformal flattening (c) planar triangulated domain obtained by angular flattening.

locations $\mathbf{x_i}$ for $i = 1, \ldots, n$, are obtained by adding independent normally distributed errors with mean 0 and a standard deviation 0.25 to the test function in accordance with the model (3). Examples of a test function and the level of noise are illustrated on each geometry in Figures 3 and 4, respectively.

At each simulation replicate, optimal values of the smoothing parameter λ in (2) and (4) are selected by the generalized cross validation for both the models on planar and non-planar domains, as described in [17] and [5], respectively.

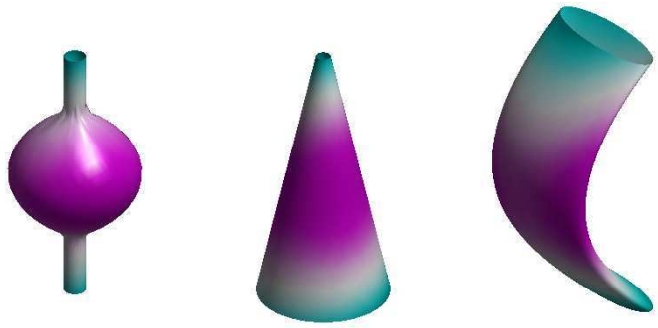

Fig. 3 Test surface domains obtained from deformation of a circular cylinder. On each surface, the color maps indicate one of the considered test functions $f(x,y,z) = a_1 \sin(2\pi x) + a_2 \sin(2\pi y) + a_3 \sin(2\pi z) + 1$, with coefficients a_1, a_2 and a_3 randomly generated from independent normal distributions with mean 1 and standard deviation 1.

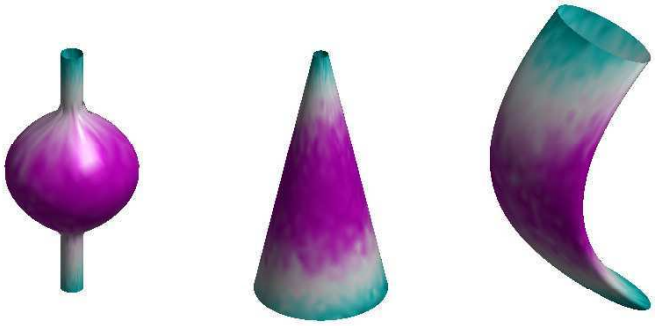

(1) (2) (3)

Fig. 4 On each test surface, at each of the data location $\mathbf{x}_i$, coinciding with the nodes of the three-dimensional meshes approximating the surface domains, independent normally distributed errors with mean 0 and a standard deviation 0.25 are added to the test function; the color maps are obtained by linear interpolation of the resulting noisy observations.

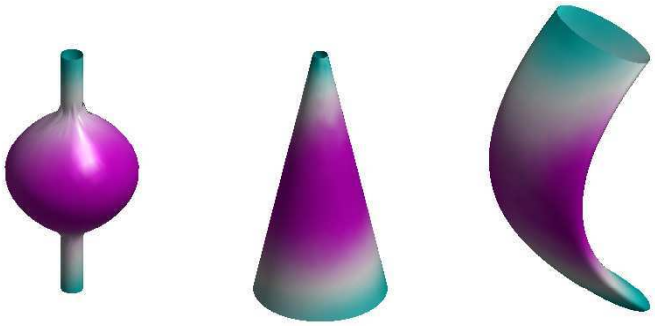

(1) (2) (3)

Fig. 5 The estimates provided by SSR over non-planar domains, with values of lambda selected by generalized cross-validation.

Table 1 shows the median and inter-quantile ranges of the Mean Square Errors (MSE) of f estimators over the 50 simulations. The table also report the results of pairwise Wilcoxon tests verifying if the distribution of MSE for the estimates provided by SSR over non-planar domains is stochastically lower than the distribution

MSE	Geometry 1	Geometry 2	Geometry 3
angular map + SSR over planar domains	0.0796(0.0335)	0.0813(0.0347)	0.1092(0.0508)
SSR over non-planar domains	0.0793(0.0339)	0.0810(0.0355)	0.0962(0.0696)
SSR over non-planar vs. SSR over planar	0.0153	7.648×10^{-07}	0.001071

Table 1 Median (inter-quantile ranges) of MSE of f estimators over the 50 simulations; p-values of pairwise Wilcoxon tests verifying if the distribution of MSE for the estimates provided by SSR over non-planar domains is stochastically lower than the distribution of the MSE for the estimates provided by SSR method over planar domains.

of the MSE for the estimates provided by SSR method over planar domains. The p-values of these tests show that the MSE of SSR over non-planar domains estimates are significantly lower than the ones of SSR over planar domains, uniformly over the three considered surface domains. Figure 5 displays the estimates provided by SSR over non-planar domains for the test functions shown in Figure 3 with added noise shown in Figure 4.

4.2 Application to hemodynamic data

This section applies the proposed smoothing technique over non-planar domains to the modeling of the hemodynamic data described in Section 2. Figure 6 displays the planar triangulated domain obtained from the three-dimensional triangulated artery wall, via computation of the conformal map. Notice the area close to the "Outflow" side where the flattened mesh is very fine; this corresponds to the aneurysm sac; recall that the aneurysm sac has to be removed from the domain when using the simpler angular map. Figure 6 shows the estimate of wall shear stress modulus obtained with SSR over non-planar domains with smoothing parameter $\lambda = 0.1$. The obtained patient-specific estimates can then be used for statistical analysis between patients, in order to detect recurrent hemodynamic patterns, common across patients, and relate them to presence and location of the pathology, and to rupture risk. Notice that this also requires appropriate registration of the patient-specific internal carotid artery geometries.

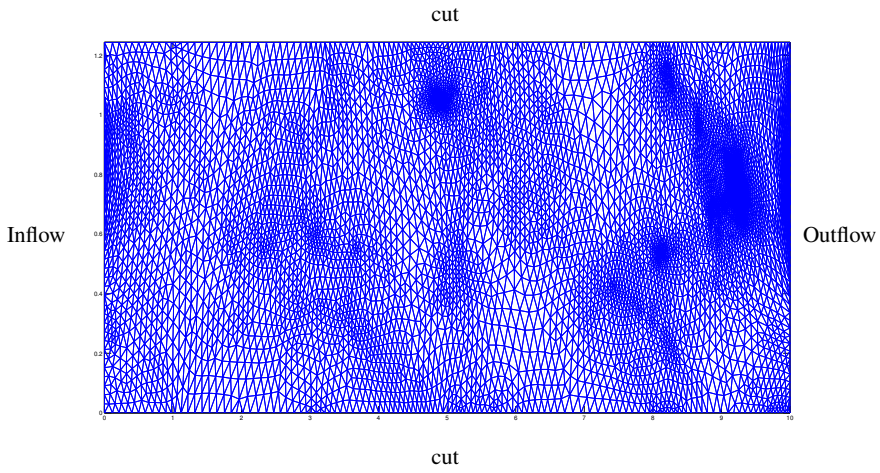

Fig. 6 Planar triangulation generated via the conformal flattening of the mesh associated with internal carotid artery in Figure 7. The sides of the planar triangulation are labeled to correspond with Figure 7. In particular, the sides of the planar triangulation labeled with "Inflow" and "Outflow" correspond to the open ends of the carotid artery. The sides indicated by "cut" correspond to a longitudinal cut along the artery wall, connecting the open boundaries of the artery.

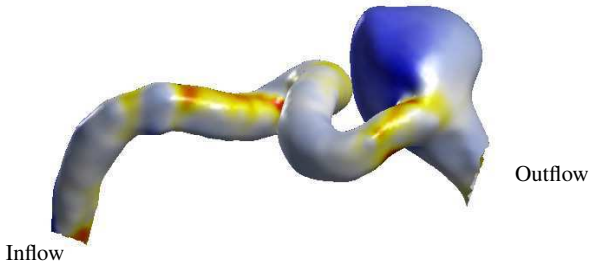

Fig. 7 Estimate of wall shear stress modulus at the systolic peak obtained with SSR over non-planar domains with smoothing parameter $\lambda = 10$.

5 Conclusion and future developments

The goal pursued in this paper has been to check the capabilities of SSR over non-planar surfaces. The simple simulation study here reported provides first evidence of the good properties of the proposed model, showing that SSR over non-planar domains provide better estimates than those obtained by first flattening the domain via an angular map and then applying SSR over the flattened domain without accounting for the domain deformation.

Within the framework of the proposed SSR model over non-planar domains it is also possible to include spatially distributed covariates, similarly to what done in [17]. In the application to hemodynamics data, this, for instance, would allow the inclusion of the values of blood pressure observed over the artery wall; pressure could thus be used as a control variable, studying also the relationship between pressure and wall-shear stress, and evaluating how this affects aneurysm pathogenesis. Moreover, as described in [17], it is possible to impose different conditions at the boundary of the domain of interest.

Another application for the proposed model is, e.g., the identification of areas of activation for hemodynamics signals over a cortical surface. The cortical surface is a sophisticated geometry that serves as the domain of the signal. A finite element method for conformally flattening the cortical surface in shown in [1]; the proposed SSR model for non-planar domains could thus be used also for this application.

The proposed models have been implemented in R [12] and Matlab. Both code versions, fully integrated with the fda packages in R [16] and Matlab, shall be released shortly.

Acknowledgements Funding by MIUR *FIRB Futuro in Ricerca* research project "Advanced statistical and numerical methods for the analysis of high dimensional functional data in life sciences and engineering", and by the program Dote Ricercatore Politecnico di Milano - Regione Lombardia, research project "Functional data analysis for life sciences".

References

1. Angenent, S., Haker, S., Tannenbaum, A., and Kikinis R., (1999) "On the Laplace-Beltrami Operator and Brain Surface Flattening", *IEEE Transactions on Medical Imaging,* 18, 700-701.
2. Boneschi, A. (2010), "Functional Data Analysis of CFD Simulations: the Systolic Wall Shear Stress Map of the Internal Carotid Artery," Master Thesis. Dipartimento di Matematica "F.Brioschi," Politecnico di Milano, Italy. Available at http://mox.polimi.it/it/progetti/pubblicazioni/tesi/boneschi.pdf
3. Chung, M.K., Robbins, S.M., Dalton, K.M., Davidson, R.J., Alexander, A.L., Evans, A.C. (2005), "Cortical thickness analysis in autism with heat kernel smoothing," *NeuroImage,* 25, 1256-1265.
4. Dierkes, U., Hildebrant, S., K*ü*ster, A., and Wohlrab, O. (1992), "Minimal Surfaces (I)", *Springer-Verlag*, Berlin.
5. Ettinger, B.D., Perotto, S., Sangalli, L.M. (2012), "Spatial smoothing over non-planar domains," in preparation.
6. Hagler, D. J., Saygin, A. P., and Sereno, M. I. (2006), " Smoothing and cluster thresholding for cortical surface-based group analysis of fMRI data," *NeuroImage,* 33, 1093-1103.
7. Haker, S., Angenent, S., Tannenbaum, A., Kikinis, R. (2000), " Nondistorting flattening maps and the 3-D visualization of colon CT images", *IEEE Trans. Med. Imag.,* 19, 665-670.
8. Piccinelli, M., Veneziani, A., Steinman, D.A., Remuzzi, A., Antiga, L. (2009), "A framework for geometric analysis of 852 vascular structures: applications to cerebral aneurysms," *IEEE Trans. Med. Imaging,* 28, 8, 1141–1155.
9. Passerini, T. (2009), "Computational hemodynamics of the cerebral circulation: multiscale modeling from the circle of Willis to cerebral aneurysms," PhD Thesis. Dipartimento di Matematica, Politecnico di Milano, Italy. Available at http://mathcs.emory.edu/.
10. Passerini, T., Sangalli, L.M., Vantini, S., Piccinelli, M., Bacigaluppi, S., Antiga, L., Boccardi, E., Secchi, P., and Veneziani, V. (2012), "An Integrated Statistical Investigation of Internal Carotid Arteries of Patients affected by Cerebral Aneurysms," *Cardiovascular Engineering and Technology*, Vol. 3, No.1, pp. 26-40.
11. Quarteroni, A. (2009), "Numerical models for differential problems", vol. 2 of *MS&A. Modeling, Simulation and Applications*, Springer-Verlag Italia, Milan.
12. R Development Core Team (2010), "R: A Language and Environment for Statistical Computing", *R Foundation for Statistical Computing*, Vienna, Austria, http://www.R-project.org.
13. Ramsay, J.O., and Ramsay, T.O., and Sangalli, L.M. (2011a), "Spatial Functional Data Analysis," in *Recent Advances in Functional Data Analysis and Related Topics,* Contributions to Statistics, Physica-Verlag Springer, 269–276.
14. Ramsay, J.O., and Ramsay, T.O., and Sangalli, L.M. (2011b), "Spatial spline regression models for data distributed over irregularly shaped regions," Proceedings of S.Co.2011 Conference. Available at http://sco2011.stat.unipd.it.
15. Ramsay, T. (2002), "Spline Smoothing over Difficult Regions," *J. R. Stat. Soc. Ser. B Stat. Methodol.*, 64, 307-319.
16. Ramsay, J.O., Wickham, H., Graves, S., Hooker, G. (2010), "fda: Functional Data Analysis", R package version 2.2.5, http://CRAN.R-project.org/package=fda.
17. Sangalli, L.M., Ramsay, J.O., and Ramsay, T.O. (2012), "Spatial Spline Regression Models," Tech. rep. N. 08/2012, MOX, Dipartimento di Matematica "F.Brioschi," Politecnico di Milano, Available at http://mox.polimi.it/it/progetti/pubblicazioni. Submitted
18. Sangalli, L. M., Secchi, P., Vantini, S., and Veneziani, A. (2009) "A case study in exploratory functional data analysis: geometrical features of the internal carotid artery", *J. Amer. Statist. Assoc.,* 104, 37-48.

MOX Technical Reports, last issues

Dipartimento di Matematica "F. Brioschi",
Politecnico di Milano, Via Bonardi 9 - 20133 Milano (Italy)

22/2012 Ettinger, B.; Passerini, T.;Perotto, S.; Sangalli, L.M.
Regression models for data distributed over non-planar domains

21/2012 Guglielmi, A.; Ieva, F.; Paganoni, A.M.; Ruggeri, F.; Soriano, J.
Semiparametric Bayesian models for clustering and classification in presence of unbalanced in-hospital survival

20/2012 Ieva, F.; Paganoni, A. M.; Zanini, P.
Statistical models for detecting Atrial Fibrillation events

19/2012 Faggiano, E.; Antiga, L.; Puppini, G.; Quarteroni, A.; Luciani G.B.; Vergara, C.
Helical Flows and Asymmetry of Blood Jet in Dilated Ascending Aorta with Normally Functioning Bicuspid Valve

18/2012 Formaggia, L.; Vergara, C.
Prescription of general defective boundary conditions in fluid-dynamics

17/2012 Manzoni, A.; Quarteroni, A.; Gianluigi Rozza, G.
Computational reduction for parametrized PDEs: strategies and applications

16/2012 Cutri', E.; Zunino, P.; Morlacchi, S.; Chiastra, C.; Migliavacca, F.
Drug delivery patterns for different stenting techniques in coronary bifurcations: a comparative computational study

15/2012 Mengaldo, G.; Tricerri, P.; Crosetto,P.; Deparis, S.; Nobile, F.; Formaggia, L.
A comparative study of different nonlinear hyperelastic isotropic arterial wall models in patient-specific vascular flow simulations in the aortic arch

14/2012 Fumagalli, A.;Scotti, A.
An unfitted method for two-phase flow in fractured porous media.

13/2012 Formaggia, L.; Guadagnini, A.; Imperiali, I.; Lever, V.; Porta, G.; Riva, M.; Scotti, A.; Tamellini, L.

Global Sensitivity Analysis through Polynomial Chaos Expansion of a basin-scale geochemical compaction model